Chapter 7

Local Discontinuous Galerkin Method for Nonlinear Ginzburg-Landau Equation

Tarek Aboelenen

Additional information is available at the end of the chapter

http://dx.doi.org/10.5772/intechopen.75300

Abstract

The Ginzburg-Landau equation has been applied widely in many fields. It describes the amplitude evolution of instability waves in a large variety of dissipative systems in fluid mechanics, which are close to criticality. In this chapter, we develop a local discontinuous Galerkin method to solve the nonlinear Ginzburg-Landau equation. The nonlinear Ginzburg-Landau problem has been expressed as a system of low-order differential equations. Moreover, we prove stability and optimal order of convergence $O(h^{N+1})$ for Ginzburg-Landau equation where h and N are the space step size and polynomial degree, respectively. The numerical experiments confirm the theoretical results of the method.

Keywords: Ginzburg-Landau equation, discontinuous Galerkin method, stability, error estimates

1. Introduction

The Ginzburg-Landau equation has arisen as a suitable model in physics community, which describes a vast variety of phenomena from nonlinear waves to second-order phase transitions, from superconductivity, superfluidity, and Bose-Einstein condensation to liquid crystals and strings in field theory [1]. The Taylor-Couette flow, Bénard convection [1] and plane Poiseuille flow [2] are such examples where the Ginzburg-Landau equation is derived as a wave envelop or amplitude equation governing wave-packet solutions. In this chapter, we develop a nodal discontinuous Galerkin method to solve the nonlinear Ginzburg-Landau equation

$$\frac{\partial u}{\partial t} - (\nu + i\eta)\Delta u + (\kappa + i\zeta)|u|^2 u - \gamma u = 0, \tag{1}$$

and periodic boundary conditions and η, ζ, γ are real constants, $\nu, \kappa > 0$. Notice that the assumption of periodic boundary conditions is for simplicity only and is not essential: the method as well as the analysis can be easily adapted for nonperiodic boundary conditions.

The various kinds of numerical methods can be found for simulating solutions of the nonlinear Ginzburg-Landau problems [3–11]. The local discontinuous Galerkin (LDG) method is famous for high accuracy properties and extreme flexibility [12–20]. To the best of our knowledge, however, the LDG method, which is an important approach to solve partial differential equations, has not been considered for the nonlinear Ginzburg-Landau equation. Compared with finite difference methods, it has the advantage of greatly facilitating the handling of complicated geometries and elements of various shapes and types as well as the treatment of boundary conditions. The higher order of convergence can be achieved without many iterations.

The outline of this chapter is as follows. In Section 2, we derive the discontinuous Galerkin formulation for the nonlinear Ginzburg-Landau equation. In Section 3, we prove a theoretical result of L^2 stability for the nonlinear case as well as an error estimate for the linear case. Section 4 presents some numerical examples to illustrate the efficiency of the scheme. A few concluding remarks are given in Section 5.

2. LDG scheme for Ginzburg-Landau equation

In order to construct the LDG method, we rewrite the second derivative as first-order derivatives to recover the equation to a low-order system. However, for the first-order system, central fluxes are used. We introduce variables r, s and set

$$r = \frac{\partial}{\partial x} s, \quad s = \frac{\partial}{\partial x} u, \tag{2}$$

then, the Ginzburg-Landau problem can be rewritten as

$$\begin{aligned} &\frac{\partial u}{\partial t} - (\nu + i\eta) r + (\kappa + i\zeta)|u|^2 u - \gamma u = 0, \\ &r = \frac{\partial}{\partial x} s, \quad s = \frac{\partial}{\partial x} u. \end{aligned} \tag{3}$$

We consider problem posed on the physical domain Ω with boundary $\partial\Omega$ and assume that a nonoverlapping element D^k such that

$$\Omega = \bigcup_{k=1}^{K} D^k. \tag{4}$$

Now we introduce the broken Sobolev space for any real number r

http://dx.doi.org/10.5772/intechopen.75300

$$H^r(\Omega) = \{v \in L^2(\Omega) : \forall k = 1, 2, \ldots . K, v|_{D^k} \in H^r\left(D^k\right)\}. \tag{5}$$

We define the local inner product and $L^2\left(D^k\right)$ norm

$$(u, v)_{D^k} = \int_{D^k} uv dx, \quad \|u\|^2_{D^k} = (u, u)_{D^k}, \tag{6}$$

as well as the global broken inner product and norm

$$(u, v)_\Omega = \sum_{k=1}^{K} (u, v)_{D^k}, \quad \|u\|^2_{L^2(\Omega)} = \sum_{k=1}^{K} (u, u)_{D^k}. \tag{7}$$

We define the jumps along a normal, $\hat{n}$, as

$$[u] = \hat{n}^- u^- + \hat{n}^+ u^+. \tag{8}$$

The numerical traces (u,s) are defined on interelement faces as the central fluxes

$$u^* = \{u\} = \frac{u^+ + u^-}{2}, \quad s^* = \{s\} = \frac{s^+ + s^-}{2}. \tag{9}$$

Let us discretize the computational domain Ω into K nonoverlapping elements, $D^k = \left[x_{k-\frac{1}{2}}, x_{k+\frac{1}{2}}\right]$, $\Delta x_k = x_{k+\frac{1}{2}} - x_{k-\frac{1}{2}}$ and $k = 1, \ldots, K$. We assume $u_h, r_h, s_h \in V_k^N$ be the approximation of u, r, s respectively, where the approximation space is defined as

$$V_k^N = \left\{v : v_k \in \mathbb{P}^N\left(D^k\right), \forall D^k \in \Omega\right\}, \tag{10}$$

where $\mathbb{P}^N\left(D^k\right)$ denotes the set of polynomials of degree up to N defined on the element D^k. We define local discontinuous Galerkin scheme as follows: find $u_h, r_h, s_h \in V_k^N$, such that for all test functions $\vartheta, \phi, \varphi \in V_k^N$,

$$\begin{aligned}
&\left(\tfrac{\partial u_h}{\partial t}, \vartheta\right)_{D^k} - (\nu + i\eta)(r_h, \vartheta)_{D^k} + (\kappa + i\zeta)\left(|u_h|^2 u_h, \vartheta\right)_{D^k} - \gamma(u_h, \vartheta)_{D^k} = 0,\\
&\left(r_h, \phi\right)_{D^k} = \left(\tfrac{\partial}{\partial x} s_h, \phi\right)_{D^k},\\
&\left(s_h, \varphi\right)_{D^k} = \left(\tfrac{\partial}{\partial x} u_h, \varphi\right)_{D^k}.
\end{aligned} \tag{11}$$

Applying integration by parts to (11), and replacing the fluxes at the interfaces by the corresponding numerical fluxes, we obtain

$$\begin{aligned}
&\left(\tfrac{\partial u_h}{\partial t}, \vartheta\right)_{D^k} - (\nu + i\eta)(r_h, \vartheta)_{D^k} + (\kappa + i\zeta)\left(|u_h|^2 u_h, \vartheta\right)_{D^k} - \gamma(u_h, \vartheta)_{D^k} = 0,\\
&\left(r_h, \phi\right)_{D^k} = -\left(s_h, \phi_x\right)_{D^k} + \left(s_h^* \phi^-\right)_{k+\frac{1}{2}} - \left(s_h^* \phi^+\right)_{k-\frac{1}{2}},\\
&\left(s_h, \varphi\right)_{D^k} = -\left(u_h, \varphi_x\right)_{D^k} + \left(u_h^* \varphi^-\right)_{k+\frac{1}{2}} - \left(u_h^* \varphi^+\right)_{k-\frac{1}{2}},
\end{aligned} \tag{12}$$

we can rewrite (12) as

$$\begin{aligned}
&\left(\tfrac{\partial u_h}{\partial t}, \vartheta\right)_{D^k} - (\nu + i\eta)(r_h, \vartheta)_{D^k} + (\kappa + i\zeta)\left(|u_h|^2 u_h, \vartheta\right)_{D^k} - \gamma(u_h, \vartheta)_{D^k} = 0,\\
&\left(r_h, \phi\right)_{D^k} = -\left(s_h, \phi_x\right)_{D^k} + \left(\hat{n}.s_h^*, \phi\right)_{\partial D^k},\\
&\left(s_h, \varphi\right)_{D^k} = -\left(u_h, \varphi_x\right)_{D^k} + \left(\hat{n}.u_h^*, \varphi\right)_{\partial D^k}.
\end{aligned} \tag{13}$$

where $\hat{n}$ is simply a scalar and takes the value of +1 and -1 at the right and the left interface, respectively.

3. Stability and error estimates

In this section, we discuss stability and accuracy of the proposed scheme, for the Ginzburg-Landau problem.

3.1. Stability analysis

In order to carry out the analysis of the LDG scheme, we have the following results.

Theorem 3.1. (L^2 *stability). The solution given by the LDG method defined by* (13) *satisfies*

$$\|u_h(x, T)\|_\Omega \leq e^{-2\gamma T}\|u_0(x)\|_\Omega$$

for any $T > 0$.

Proof. Set $\left(\vartheta, \phi, \varphi\right) = (u_h, \nu u_h, \nu s_h)$ in (13) and consider the integration by parts formula $\left(u, \frac{\partial r}{\partial x}\right)_{D^k} + \left(r, \frac{\partial u}{\partial x}\right)_{D^k} = [ur]_{x_{k-\frac{1}{2}}}^{x_{k+\frac{1}{2}}}$, we get

$$\begin{aligned}
&\left((u_h)_t, u_h\right)_{D^k} + (s_h, s_h)_{D^k}\\
&= -\nu(r_h, u_h)_{D^k} + (\nu + i\eta)(r_h, u_h)_{D^k} - (\kappa + i\zeta)\left(|u_h|^2 u_h, u_h\right)_{D^k}\\
&+\gamma(u_h, u_h)_{D^k} + \nu\left(\hat{n}.s_h^*, u_h\right)_{\partial D^k} + \nu\left(\hat{n}.u_h^*, s_h\right)_{\partial D^k} - \nu(\hat{n}.s_h, u_h)_{\partial D^k}.
\end{aligned} \tag{14}$$

Taking the real part of the resulting equation, we obtain

$$\begin{aligned}
\left((u_h)_t, u_h\right)_{D^k} + (s_h, s_h)_{D^k} = &-\kappa\left(|u_h|^2 u_h, u_h\right)_{D^k} + \gamma(u_h, u_h)_{D^k}\\
&+ \nu\left(\hat{n}.s_h^*, u_h\right)_{\partial D^k} + \nu\left(\hat{n}.u_h^*, s_h\right)_{\partial D^k} - \nu(\hat{n}.s_h, u_h)_{\partial D^k}.
\end{aligned} \tag{15}$$

Removing the positive term $\kappa\left(|u_h|^2 u_h, u_h\right)_{D^k}$, we obtain

$$\left((u_h)_t, u_h\right)_{D^k} + (s_h, s_h)_{D^k} \leq \gamma\|u_h\|^2_{L^2\left(D^k\right)} + \nu\left(\hat{n}.s_h^*, u_h\right)_{\partial D^k} + \nu\left(\hat{n}.u_h^*, s_h\right)_{\partial D^k} - \nu(\hat{n}.s_h, u_h)_{\partial D^k}. \tag{16}$$

Summing over all elements (16), we easily obtain

http://dx.doi.org/10.5772/intechopen.75300

$$\left((u_h)_t, u_h\right)_{L^2(\Omega)} + (s_h, s_h)_{L^2(\Omega)} \le \gamma \|u_h\|_\Omega^2. \tag{17}$$

Employing Gronwall's inequality, we obtain

$$\|u_h(x,T)\|_\Omega \le e^{-2\gamma T}\|u_0(x)\|_\Omega. \quad \square$$

3.2. Error estimates

We consider the linear Ginzburg-Landau equation

$$\frac{\partial u}{\partial t} - (\nu + i\eta)\Delta u + (\kappa + i\zeta)u - \gamma u = 0. \tag{18}$$

It is easy to verify that the exact solution of the above (18) satisfies

$$\begin{aligned} &(u_t, \vartheta)_{D^k} - (\nu + i\eta)(r, \vartheta)_{D^k} + (\kappa + i\zeta)(u, \vartheta)_{D^k} - \gamma(u, \vartheta)_{D^k} = 0, \\ &\left(r, \phi\right)_{D^k} = -\left(s, \phi_x\right)_{D^k} + \left(\hat{n}.s^*, \phi\right)_{\partial D^k}, \\ &(s, \varphi)_{D^k} = -\left(u, \varphi_x\right)_{D^k} + (\hat{n}.u^*, \varphi)_{\partial D^k}. \end{aligned} \tag{19}$$

Subtracting (19) from the linear Ginzburg-Landau Eq. (13), we have the following error equation

$$\begin{aligned} &\left((u-u_h)_t, \vartheta\right)_{D^k} + \left(s - s_h, \phi_x\right)_{D^k} + \left(u - u_h, \varphi_x\right)_{D^k} + (\kappa + i\zeta)(u - u_h, \vartheta)_{D^k} \\ &-\gamma(u - u_h, \vartheta)_{D^k} + \left(r - r_h, \phi\right)_{D^k} + (s - s_h, \varphi)_{D^k} - \left(\hat{n}.(s - s_h)^*, \phi\right)_{\partial D^k} \\ &-(\nu + i\eta)(r - r_h, \vartheta)_{D^k} - (\hat{n}.(u - u_h)^*, \varphi)_{\partial D^k} = 0. \end{aligned} \tag{20}$$

For the error estimate, we define special projections $\mathcal{P}^-$ and $\mathcal{P}^+$ into V_h^k. For all the elements, D^k, $k = 1, 2, \ldots, K$ are defined to satisfy

$$\begin{aligned} &(\mathcal{P}^+u - u, v)_{D^k} = 0, \quad \forall v \in \mathbb{P}_N^k(D^k), \quad \mathcal{P}^+u\left(x_{k-\frac{1}{2}}\right) = u\left(x_{k-\frac{1}{2}}\right), \\ &(\mathcal{P}^-u - u, v)_{D^k} = 0, \quad \forall v \in \mathbb{P}_N^{k-1}(D^k), \quad \mathcal{P}^-u\left(x_{k+\frac{1}{2}}\right) = u\left(x_{k+\frac{1}{2}}\right). \end{aligned} \tag{21}$$

Denoting

$$\begin{aligned} &\pi = \mathcal{P}^-u - u_h, \quad \pi^e = \mathcal{P}^-u - u, \quad \varepsilon = \mathcal{P}^+r - r_h, \quad \varepsilon^e = \mathcal{P}^+r - r, \\ &\tau = \mathcal{P}^+s - s_h, \quad \tau^e = \mathcal{P}^+s - s. \end{aligned} \tag{22}$$

For the abovementioned special projections, we have, by the standard approximation theory [21], that

$$\begin{aligned} &\|\mathcal{P}^+u(.) - u(.)\|_{L^2(\Omega_h)} \le Ch^{N+1}, \\ &\|\mathcal{P}^-u(.) - u(.)\|_{L^2(\Omega_h)} \le Ch^{N+1}, \end{aligned} \tag{23}$$

where here and below C is a positive constant (which may have a different value in each occurrence) depending solely on u and its derivatives but not of h.

Theorem 3.2. *Let u be the exact solution of the problem* (18)*, and let u_h be the numerical solution of the semi-discrete LDG scheme* (13)*. Then for small enough h, we have the following error estimates:*

$$\|u(.,t) - u_h(.,t)\|_{L^2(\Omega_h)} \leq Ch^{N+1}, \tag{24}$$

where the constant C is dependent upon T and some norms of the solutions.

Proof. From the Galerkin orthogonality (20), we get

$$\begin{aligned}&\left((\pi-\pi^e)_t,\vartheta\right)_{D^k}+\left(\tau-\tau^e,\phi_x\right)_{D^k}+\left(\pi-\pi^e,\varphi_x\right)_{D^k}+(\kappa+i\zeta)(\pi-\pi^e,\vartheta)_{D^k}-\gamma(\pi-\pi^e,\vartheta)_{D^k}\\&+\left(\varepsilon-\varepsilon^e,\phi\right)_{D^k}+(\tau-\tau^e,\varphi)_{D^k}+\left(\phi-\phi^e,\beta\right)_{D^k}-\left(\hat{n}.(\tau-\tau^e)^*,\phi\right)_{\partial D^k}-(\nu+i\eta)\\&\times(\varepsilon-\varepsilon^e,\vartheta)_{D^k}-(\hat{n}.(\pi-\pi^e)^*,\varphi)_{\partial D^k}=0.\end{aligned} \tag{25}$$

Taking the real part of the resulting equation, we obtain

$$\begin{aligned}&\left((\pi-\pi^e)_t,\vartheta\right)_{D^k}+\left(\tau-\tau^e,\phi_x\right)_{D^k}+\left(\pi-\pi^e,\varphi_x\right)_{D^k}+\kappa(\pi-\pi^e,\vartheta)_{D^k}\\&-\gamma(\pi-\pi^e,\vartheta)_{D^k}+\left(\varepsilon-\varepsilon^e,\phi\right)_{D^k}+(\tau-\tau^e,\varphi)_{D^k}-\left(\hat{n}.(\tau-\tau^e)^*,\phi\right)_{\partial D^k}\\&-\nu(\varepsilon-\varepsilon^e,\vartheta)_{D^k}-(\hat{n}.(\pi-\pi^e)^*,\varphi)_{\partial D^k}=0.\end{aligned} \tag{26}$$

We take the test functions

$$\vartheta=\pi,\quad \phi=\nu\pi,\quad \varphi=\nu\tau, \tag{27}$$

we obtain

$$\begin{aligned}&\left((\pi-\pi^e)_t,\pi\right)_{D^k}+\nu(\tau-\tau^e,\pi_x)_{D^k}+\nu(\pi-\pi^e,\tau_x)_{D^k}\\&+\kappa(\pi-\pi^e,\pi)_{D^k}-\gamma(\pi-\pi^e,\pi)_{D^k}+\nu(\varepsilon-\varepsilon^e,\pi)_{D^k}\\&+\nu(\tau-\tau^e,\tau)_{D^k}-\nu(\hat{n}.(\tau-\tau^e)^*,\pi)_{\partial D^k}-\nu(\varepsilon-\varepsilon^e,\pi)_{D^k}-\nu(\hat{n}.(\pi-\pi^e)^*,\tau)_{\partial D^k}=0.\end{aligned} \tag{28}$$

Summing over k, simplify by integration by parts and (9), we get

$$\begin{aligned}&(\pi_t,\pi)_\Omega+\nu(\tau,\tau)_\Omega=\nu(\tau^e,\pi_x)_\Omega+\nu(\pi^e,\tau_x)_\Omega+(\pi_t^e,\pi)_\Omega-\gamma(\pi^e,\pi)_\Omega+\kappa(\pi^e,\pi)_\Omega\\&+\nu(\tau^e,\tau)_\Omega+\gamma(\pi,\pi)_\Omega-\kappa(\pi,\pi)_\Omega-\nu\sum_{k=1}^{K}(\hat{n}.(\pi^e)^*,\tau)_{\partial D^k}-\nu\sum_{k=1}^{K}(\hat{n}.(\tau^e)^*,\pi)_{\partial D^k},\end{aligned} \tag{29}$$

we can rewrite (29) as

$$(\pi_t,\pi)_\Omega+\nu(\tau,\tau)_\Omega=I+II+III, \tag{30}$$

where

$$I=\nu(\tau^e,\pi_x)_\Omega+\nu(\pi^e,\tau_x)_\Omega, \tag{31}$$

$$\begin{aligned}II=&\left(\pi_t^e,\pi\right)_\Omega-\gamma(\pi^e,\pi)_\Omega+\kappa(\pi^e,\pi)_\Omega+\nu(\tau^e,\tau)_\Omega\\&-\nu\sum_{k=1}^{K}(\hat{n}.(\pi^e)^*,\tau)_{\partial D^k}-\nu\sum_{k=1}^{K}(\hat{n}.(\tau^e)^*,\pi)_{\partial D^k},\end{aligned} \tag{32}$$

$$III = \gamma(\pi, \pi)_\Omega - \kappa(\pi, \pi)_\Omega. \tag{33}$$

Using the definitions of the projections $\mathcal{P}, \mathcal{S}$ (21) in (31), we get

$$I = 0. \tag{34}$$

From the approximation results (23) and Young's inequality in (32), we obtain

$$II \le c_1 \|\pi\|^2_{L^2(\Omega)} + c_2 \|\tau\|^2_{L^2(\Omega)} + Ch^{2N+2}. \tag{35}$$

and

$$III \le c_1 \|\pi\|^2_{L^2(\Omega)}. \tag{36}$$

Combining (34), (35), (36) and (30), we obtain

$$(\pi_t, \pi)_\Omega + \nu(\tau, \tau)_\Omega \le c_1 \|\pi\|^2_{L^2(\Omega)} + c_2 \|\tau\|^2_{L^2(\Omega)} + Ch^{2N+2}, \tag{37}$$

provided c_2 is sufficiently small such that $c_2 \le \nu$, we obtain that

$$(\pi_t, \pi)_\Omega \le c_1 \|\pi\|^2_{L^2(\Omega)} + Ch^{2N+2}. \tag{38}$$

From the Gronwall's lemma and standard approximation theory, the desired result follows. □.

4. Numerical examples

In this section, we present several numerical examples to illustrate the previous theoretical results. We use the high-order Runge-Kutta time discretizations [22], when the polynomials are of degree N, a higher order accurate Runge-Kutta (RK) method must be used in order to guarantee that the scheme is stable. In this chapter, we use a fourth-order non-total variation diminishing (TVD) Runge-Kutta scheme [23]. Numerical experiments demonstrate its numerical stability

$$\frac{\partial \mathbf{u}_h}{\partial t} = \mathcal{F}(\mathbf{u}_h, t), \tag{39}$$

where $\mathbf{u}_h$ is the vector of unknowns, we can use the standard fourth-order four-stage explicit RK method (ERK)

$$\begin{aligned}
\mathbf{k}^1 &= \mathcal{F}(\mathbf{u}_h^n, t^n), \\
\mathbf{k}^2 &= \mathcal{F}\left(\mathbf{u}_h^n + \frac{1}{2}\Delta t \mathbf{k}^1, t^n + \frac{1}{2}\Delta t\right), \\
\mathbf{k}^3 &= \mathcal{F}\left(\mathbf{u}_h^n + \frac{1}{2}\Delta t \mathbf{k}^2, t^n + \frac{1}{2}\Delta t\right), \\
\mathbf{k}^4 &= \mathcal{F}(\mathbf{u}_h^n + \Delta t \mathbf{k}^3, t^n + \Delta t), \\
\mathbf{u}_h^{n+1} &= \mathbf{u}_h^n + \frac{1}{6}(\mathbf{k}^1 + 2\mathbf{k}^2 + 2\mathbf{k}^3 + \mathbf{k}^4),
\end{aligned} \tag{40}$$

to advance from $\mathbf{u}_h^n$ to $\mathbf{u}_h^{n+1}$, separated by the time step, Δt. In our examples, the condition $\Delta t \leq C\Delta x_{min}^{\alpha}$ $(0 < C < 1)$ is used to ensure stability.

Example 4.1 *We consider the following linear Ginzburg-Landau equation*

$$\frac{\partial u}{\partial t} - (\nu + i\eta)\Delta u + (\kappa + i\zeta)u = 0, \quad x \in [-20, 20], \quad t \in (0, 0.5], \quad u(x, 0) = u_0(x), \tag{41}$$

with

$$\eta = \frac{1}{2}, \kappa = -\frac{\nu\left(3\sqrt{1+4\nu^2} - 1\right)}{2(2+9\nu^2)}, \zeta = -1, \gamma = 0. \tag{42}$$

The exact solution $u(x,t) = a(x)e^{id\ln(a(x)) - i\omega t}$ where

$$a(x) = Fsech(x), F = \sqrt{\frac{d\sqrt{1+4\nu^2}}{-2\kappa}}, d = \frac{\sqrt{1+4\nu^2} - 1}{2\nu}, \omega = -\frac{d\left(1+4\nu^2\right)}{2\nu}. \tag{43}$$

The convergence rates and the numerical L^2 error are listed in **Figure 1** for several different values of ν, confirming optimal $O\left(h^{N+1}\right)$ order of convergence across.

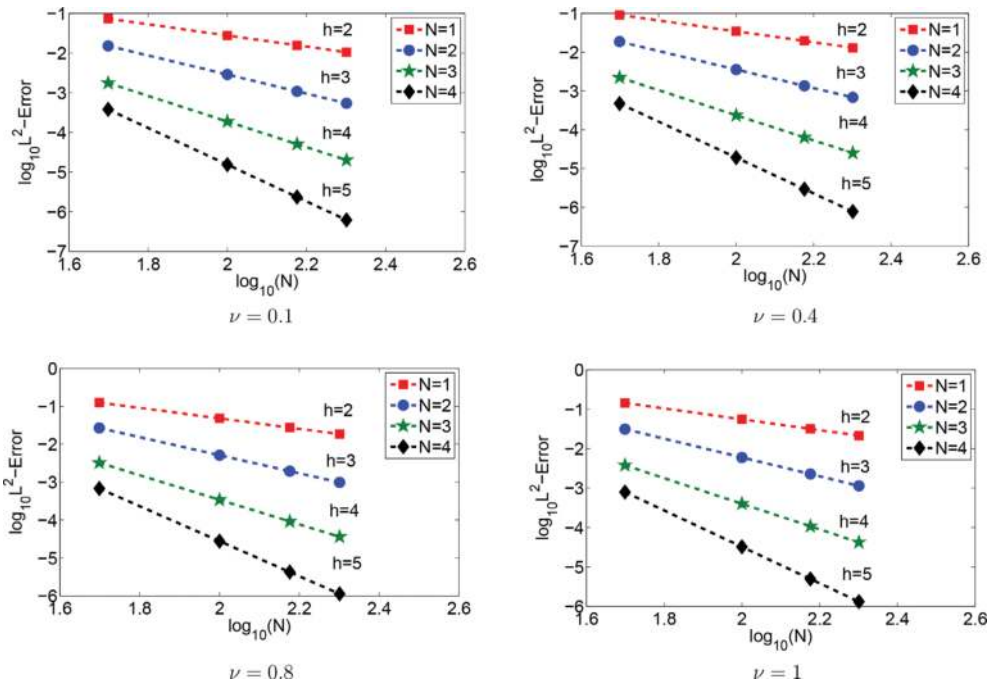

Figure 1. The rate of convergence for the solving the nonlinear Ginzburg-Landau equation in Example 4.2.

http://dx.doi.org/10.5772/intechopen.75300

Example 4.2 *We consider the nonlinear Ginzburg-Landau Eq.* (1) *with initial condition,*

$$u(x,0) = e^{-x^2}, \tag{44}$$

with parameters $\nu = 1, \kappa = 1, \eta = 1, \zeta = 2,\ x \in [-10, 10]$. We consider cases with $N = 2$ and $K = 40$ and solve the equation for several different values of γ. The numerical solution $u_h(x,t)$ for $\gamma = 2, 1, 0, -1, -2$ is shown in **Figures 2** and **3**. The parameter γ will affect the wave shape. From these figures, it is obvious that the solution decays rapidly with time evolution especially for $\gamma < 0$ and the parameter γ dramatically affects the wave shape.

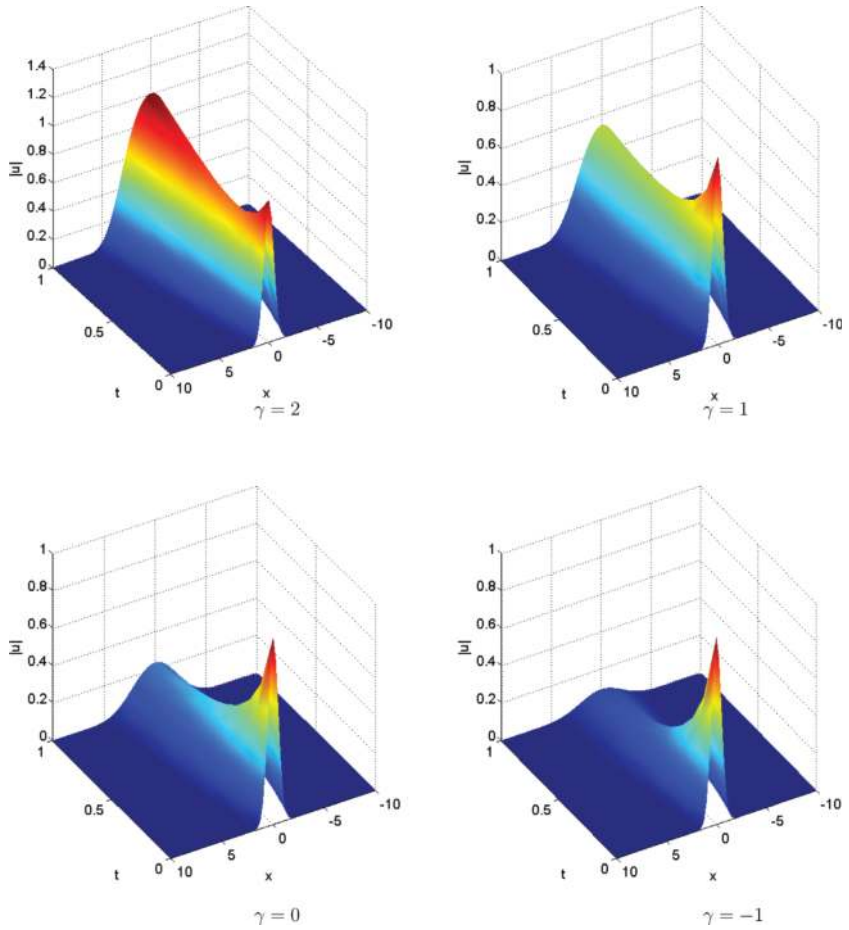

Figure 2. Numerical results for the nonlinear Ginzburg-Landau equation in Example 4.2.

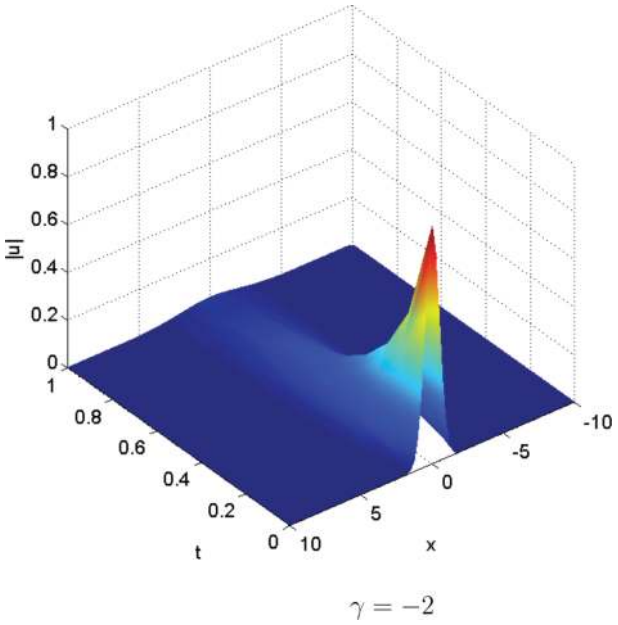

Figure 3. Numerical results for the nonlinear Ginzburg-Landau equation with $\gamma = -2$ in Example 4.2.

5. Conclusions

In this chapter, we developed and analyzed a local discontinuous Galerkin method for solving the nonlinear Ginzburg-Landau equation and have proven the stability of this method. Numerical experiments confirm that the optimal order of convergence is recovered. As a last example, the Ginzburg-Landau equation with initial condition is solved for different values of γ and results show that the parameter γ dramatically affects the wave shape. In addition, the solution decays rapidly with time evolution especially for γ<0.

Author details

Tarek Aboelenen

Address all correspondence to: tarek.aboelenen@aun.edu.eg

Department of Mathematics, Assiut University, Assiut, Egypt

References

[1] Aranson IS, Kramer L. The world of the complex Ginzburg-Landau equation. Reviews of Modern Physics. 2002;**74**:99

[2] Stewartson K, Stuart J. A non-linear instability theory for a wave system in plane Poiseuille flow. Journal of Fluid Mechanics. 1971;**48**:529-545

[3] Wang T, Guo B. Analysis of some finite difference schemes for two-dimensional Ginzburg-landau equation. Numerical Methods for Partial Differential Equations. 2011; **27**:1340-1363

[4] Shokri A, Dehghan M. A meshless method using radial basis functions for the numerical solution of two-dimensional complex Ginzburg-Landau equation. Computer Modeling in Engineering and Sciences. 2012;**84**:333

[5] Wang H. An efficient Chebyshev–Tau spectral method for Ginzburg–Landau–Schrödinger equations. Computer Physics Communications. 2010;**181**:325-340

[6] Chen Z. Mixed finite element methods for a dynamical Ginzburg-Landau model in superconductivity. Numerische Mathematik. 1997;**76**:323-353

[7] Gao H, Li B, Sun W. Optimal error estimates of linearized Crank-Nicolson Galerkin FEMs for the time-dependent Ginzburg–Landau equations in superconductivity. SIAM Journal on Numerical Analysis. 2014;**52**:1183-1202

[8] Wang S, Zhang L. An efficient split-step compact finite difference method for cubic–quintic complex Ginzburg–Landau equations. Computer Physics Communications. 2013;**184**:1511-1521

[9] Wang T, Guo B. A robust semi-explicit difference scheme for the Kuramoto–Tsuzuki equation. Journal of Computational and Applied Mathematics. 2009;**233**:878-888

[10] Hao Z-P, Sun Z-Z, Cao W-R. A three-level linearized compact difference scheme for the Ginzburg–Landau equation. Numerical Methods for Partial Differential Equations. 2015; **31**:876-899

[11] Shokri A, Afshari F. High-order compact ADI method using predictor–corrector scheme for 2D complex Ginzburg–landau equation. Computer Physics Communications. 2015; **197**:43-50

[12] Arnold DN, Brezzi F, Cockburn B, Marini LD. Unified analysis of discontinuous Galerkin methods for elliptic problems. SIAM Journal on Numerical Analysis. 2002;**39**:1749-1779

[13] Hesthaven JS, Warburton T. Nodal Discontinuous Galerkin Methods: Algorithms, Analysis, and Applications. 1st ed. New York: Springer Publishing Company, Incorporated; 2007

[14] Bernardo Cockburn C-WS, Karniadakis GE. Discontinuous Galerkin Methods: Theory, Computation and Applications. 1st ed. New York: Springer; 2000

[15] El-Tantawy S, Aboelenen T. Simulation study of planar and nonplanar super rogue waves in an electronegative plasma: Local discontinuous Galerkin method. Physics of Plasmas. 2017;**24**:052118

[16] Yan J, Shu C-W. Local discontinuous Galerkin methods for partial differential equations with higher order derivatives. Journal of Scientific Computing. 2002;**17**:27-47

[17] Aboelenen T. Local discontinuous Galerkin method for distributed-order time and space-fractional convection–diffusion and Schrödinger-type equations. Nonlinear Dynamics. 2017:1-19

[18] Aboelenen T. A high-order nodal discontinuous Galerkin method for nonlinear fractional Schrödinger type equations. Communications in Nonlinear Science and Numerical Simulation. 2018;**54**:428-452

[19] Aboelenen T, El-Hawary H. A high-order nodal discontinuous Galerkin method for a linearized fractional Cahn–Hilliard equation. Computers & Mathematics with Applications. 2017;**73**:1197-1217

[20] Aboelenen T. Discontinuous Galerkin methods for fractional elliptic problems; 2018. arXiv preprint arXiv:1802.02327

[21] Ciarlet PG. Finite Element Method for Elliptic Problems. Philadelphia, PA, USA: Society for Industrial and Applied Mathematics; 2002

[22] Cockburn B. High-Order Methods for Computational Physics, Berlin, Heidelberg: Springer; 1999. pp. 69-224. DOI: 10.1007/978-3-662-03882-6_2

[23] Gottlieb S, Shu C-W. Total variation diminishing Runge-Kutta schemes. Mathematics of Computation. 1998;**67**:73-85